Engineering Journal of the University of Qatar, Vol. 16, 2003, pp.73-86

DIFFERENTIAL AMPLITUDE PHASE SHIFT KEYING (DAPSK): A NEW MODULATION METHOD FOR A TURBO CODE IN DIGITAL RADIO BROADCASTING

Khalid H. Sayhood[1] and Wu Le Nan[2]
Radio Engineering Department
Southeast University
Nanjing 210096
P. R. CHINA
[1]E–mail: khsay57@yahoo.com, [2]E–mail: wuln@seu.edu.cn

ABSTRACT

The multilevel modulation techniques of M–Differential Amplitude Phase Shift Keying (DAPSK) have been proposed in combination with Turbo code scheme for digital radio broadcasting bands below 30 MHz radio channel. Comparison of this modulation method with channel coding in an Additive White Gaussian Noise (AWGN) and multi–path–fading channels has been presented. The analysis provides an iterative decoding of the Turbo code.

Keywords: DAPSK system, Turbo code, digital radio broadcasting

I. INTRODUCTION

For digital radio broadcasting below 30 MHz, a standard transmission system has been specified in [1]. This system has to cope with multi–path propagation channels in realistic radio environment. The effect of frequency–selective fading, which means that some of the paths strongly affect the radio channel, must be taken into account. Therefore, an efficient channel–coding scheme has to be used. Since hard decision decoding effectively reduces the distance of a code by a factor of two [2], soft decision decoding has to be applied in order to achieve good performance.

16 and 64–Quadrature Amplitude Modulation (QAM) are two candidates that have been proposed as modulation schemes for digital radio broadcasting application [3]. QAM is a coherent modulation technique that makes necessary the transmission of pilot signals for the channel estimation. An equalizer must be implemented which leads to an increased computation complexity in the receiver. As an alternative, a multilevel purely differential modulation technique, M–Differential Amplitude Phase Shift Keying (DAPSK) has been developed, which does not require any pilot symbols, channel estimation or equalization. An entire description of M–DAPSK in the un–coded case can be found in Appendix 1. For realistic comparison of these modulation techniques, the channel–coding scheme should be taken into account because the performance of soft decision decoding depends on the modulation technique. Therefore, the objective of this paper is to analyze the performance in the coded case [4]–[6].

Turbo codes are a class of forward error correction codes that offer energy efficiencies close to the limits predicted by information theory [7]. The features of Turbo codes include parallel code concatenation, recursive convolution encoding, non–uniform interleaving and an associated iterative decoding algorithm. Although the iterative decoding algorithm has been primarily used for the decoding of Turbo codes, it represents a solution to a more general class of estimation problems such as: a data set directly or indirectly drives the state transitions of two or more Markov process. The output of one or more of the Markov processes is observed through noise; based on the observations, the original data set is estimated. Turbo codes can operate at low Signal–to–Noise Ratios (SNR) because the number of low weight code words is small [8]. The process of phase estimation and tracking becomes difficult to perform. Additionally, Turbo–decoding requires precise estimates of the channel gain and noise variance. A punctured convolution code proposed in [1] that has its bit error probability compared with Turbo code with similar decoding complexity (see Appendix 2) is not favorable. As far as we know, no proposal of Turbo code for DAPSK modulation has been made before as both DAPSK modulation and the Turbo code technique itself is rather new. Therefore, Turbo coded with DAPSK modulation has been analyzed.

This paper is structured as follows. The performance of DAPSK modulation on various ring factors is described in Sec. II. In Sec. III, the error performance of coded system in a noisy channel is described. Numerical results for different information bit rates and channel coding bit rates are shown and discussed in Sec. IV over the same channel bandwidth. Finally, conclusions are drawn in Sec. V.

II. PERFORMANCE WITH RING FACTORS

The performance of Turbo–coded modulated 16–DAPSK depends to great extent on the choice of the amplitude factor α. This dependency is plotted in Fig. 1 for different signal–to–noise ratio per bit E_b/N_o and different channel conditions for a Turbo–coded system of code rate 1/3. The optimal amplitude factor slightly depends on E_b/N_o and is approximately $\alpha_{optimum} = 1.3$ for an Additive White Gaussian Noise (AWGN) and $\alpha_{optimum} = 1.4$ for frequency–selective Rayleigh fading channels. The ring factor that minimizes the bit error rate will be true optimal ring factor of this modulation scheme because optimal thresholds are also a function of ring factor. An optimal ring factor occurs since the phase error probability increases when the ring factor is high and the amplitude error probability increases when the ring factor is low. This is because for fixed E_b/N_o, the size of the inner ring decreases with increasing ring factor and hence the signal points in that ring become closer together, thus the increase in error probability.

The optimal ring factor for circular 16–DAPSK as function of normalized maximum Doppler frequency f_{Dsh} (see Appendix 3) and average received E_b/N_o is shown in Fig. 2. The results indicate that for specific values of $f_{Dsh}T_s$, where T_s is the bit period, lower optimal ring factors can be obtained when lower E_b/N_o is applied. Physically, either at high E_b/N_o or at high $f_{Dsh}T_s$, the error in the system is dominated by the random FM noise, which changes the phase of the received signal rapidly. Hence, the variation of ring factor does not affect the error of the phase. At high $f_{Dsh}T_s$, the optimal ring factor of the modulation scheme will be higher than at low $f_{Dsh}T_s$. Therefore, the amplitude differential decoder can correctly decode the received signal even at lower ring factors and the received phase is less affected by random FM noise.

III. ERROR PERFORMANCES IN NOISY CHANNEL

Computer simulations were performed in order to make quantitative comparisons of the different multilevel modulation schemes (16–QAM, 8–DAPSK and 16–DAPSK) in an AWGN and frequency–selective Rayleigh fading channels. The comparative analysis of differential modulation/demodulation techniques considers the measurements and estimation of the channel characteristics. The channel model is described in Appendix 3.

1. AWGN Channel

The performance of the three considered modulation schemes in an AWGN channel is presented in Fig. 3. Puncturing is used to increase the code rate to 1/2. For the interpretation of the simulation results, we concentrate on the essential E_b/N_o that guarantees a Bit Error Rate (BER) of 10^{-5}. Figure 3 demonstrates the performance of 16–DAPSK–modulations. This comparison shows that a differential modulation technique that has a 16–DAPSK has a poor performance and it is not suitable for the considered digital radio broadcasting application. Since it requires an additional of about 2 dB in E_b/N_o for the same transmission quality compared with 16–QAM performance. A fundamental performance improvement shows the BER curve for 8–DAPSK modulation. This differential modulation scheme reduces the above–mentioned 2 dB differences in E_b/N_o to a value of approximately 0.5 dB. The simulation results in an AWGN channel show an advantage of approximately 2 dB in E_b/N_o for the 16–QAM modulation in comparison to the 16–DAPSK modulation techniques. However, there are some advantages in the computation complexity of 16–DAPSK receivers, which is the main motivation for this suggestion. The performance of 16–QAM with punctured convolution code as proposed in [1] is shown on the same figure under the same total bit

rates for the purpose of comparisons for the two systems. For code rate of 1/2 (for example) as shown in Fig. 3(b), the performance of 16–DAPSK with Turbo code requires an additional 3.4 dB in E_b/N_o compared with 16–QAM with punctured convolution code under the same BER. This means that there is about 1 dB penalty compared with the system in [1]. The punctured convolution code of [1] has 1/4–mother code rate and a constraint length of 7. The octal forms of the generator polynomials are 133, 171, 145 and 133.

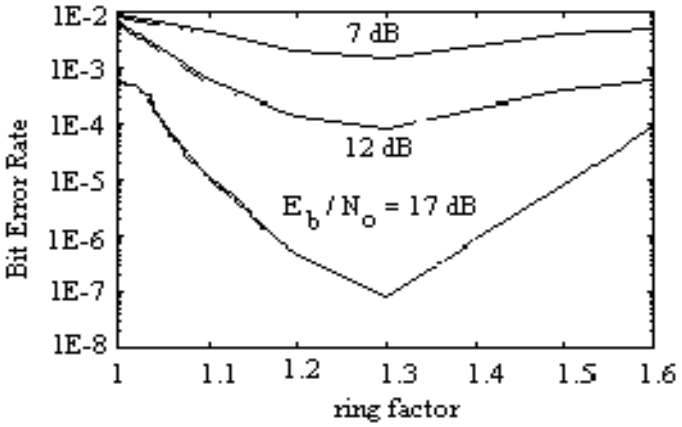

(a) AWGN channel

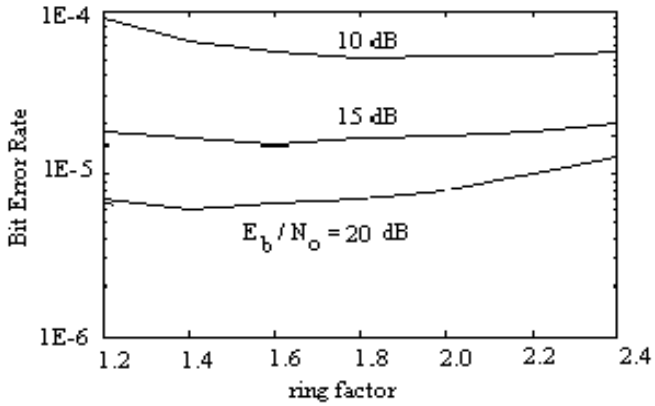

(b) Frequency–selective Rayleigh fading channel with path 1

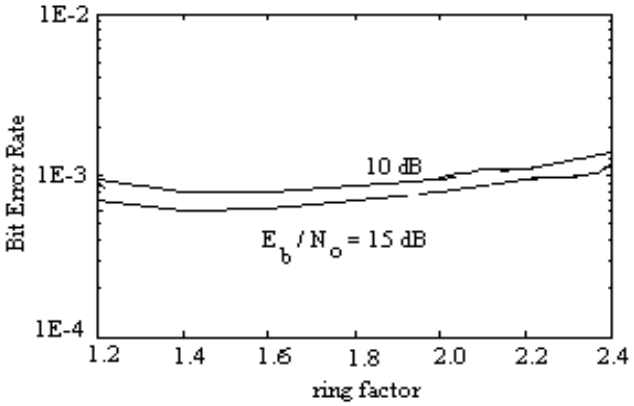

(c) frequency–selective Rayleigh fading channel with path 3

Fig. (1) Influence of the ring factor on the bit error rate of Turbo 1/3 coded with 16–DAPSK

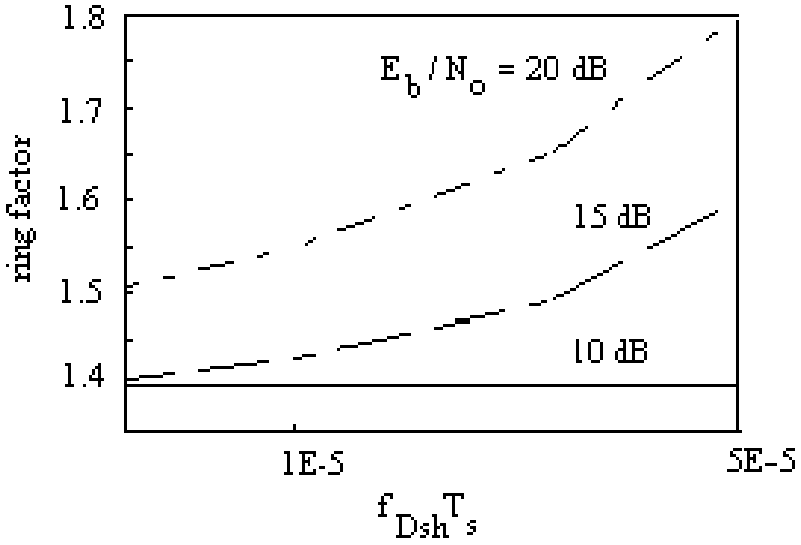

Fig. (2) Optimal ring factor of circular 16–DAPSK as function of normalized maximum Doppler frequency and E_b/N_0

2. Frequency–Selective Rayleigh fading channel

High data–rate transmission in digital radio channels has to cope with multi–path propagation that occurs especially in the case of portable receiver applications and/or reflections on moving targets within the radio channel for stationary receivers. Our simulations are based on the propagation model given in [1] and are shown in Table 3. Exact knowledge about the radio channel behavior is not yet available for digital radio broadcasting applications. The modification of the channel impulse response is arranged according to Rayleigh–distributed amplitude and uniformly distributed phase for each path of the propagation model. Figure 4 demonstrates the simulation results of 16–DAPSK techniques in frequency–selective Rayleigh fading channel. The performance in the multi–path propagation environment shows the typical characteristic of a Rayleigh fading channel. These results are valid for the coded case of rates 1/3 and 1/2. The performance for 16–QAM–modulation technique for both Turbo and punctured convolution codes [1] has been calculated in path 1 of the radio channel. We are interested in the performance comparison between the 16–QAM and the 16–DAPSK modulation technique in a frequency–selective Rayleigh fading channel and in the coded case of Turbo codes. The difference between 16–DAPSK and 16–QAM is approximately 2.5 dB for BER of 10^{-5}, for example under path 1 and for code rate of 1/3. The performance is improving as $f_{Dsh}T_s$ decreases. Clearly, 16–QAM performs better than circular 16–DAPSK. Since coherent detection performs up to 3 dB better than its differential counterpart. In addition, from the point of view of energy per bit, 16–QAM has a more efficient signal constellation than 16–DAPSK. For these modulation schemes, the relative power saving in an AWGN channel is given in [9]. However, applying coherent detection in the mobile radio environment is a very difficult task since highly accurate carrier recovery and phase tracking is required at the receiver. For systems such as 16–QAM, it is also important to accurately track the fading envelope. In practice, imperfections in these tracking circuits can seriously degrade a coherent system. This indicates the importance of selecting the proper channel model in order to accurately predict the performance of Turbo–coded system. The simulation results show that the system with lower code rate using 16–QAM with Turbo code perform better than the system using 16–QAM with punctured convolution code for almost all values of E_b/N_o of interest. To achieve BER of 10^{-5}, 16–QAM with punctured convolution code requires 3 dB in E_b/N_o higher than that for Turbo code with rates between 1/2 and 1/3. When E_b/N_o is smaller than 6 dB, only 16–QAM with punctured convolution can effect communication, because of its high error correction ability and high accumulated BER.

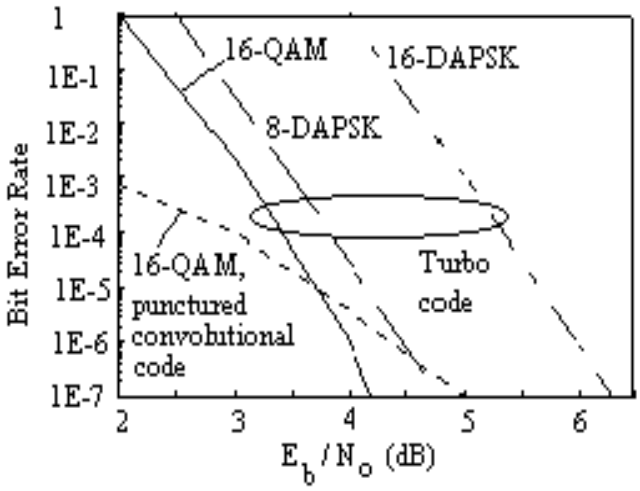

(a) Code rate = 1/3

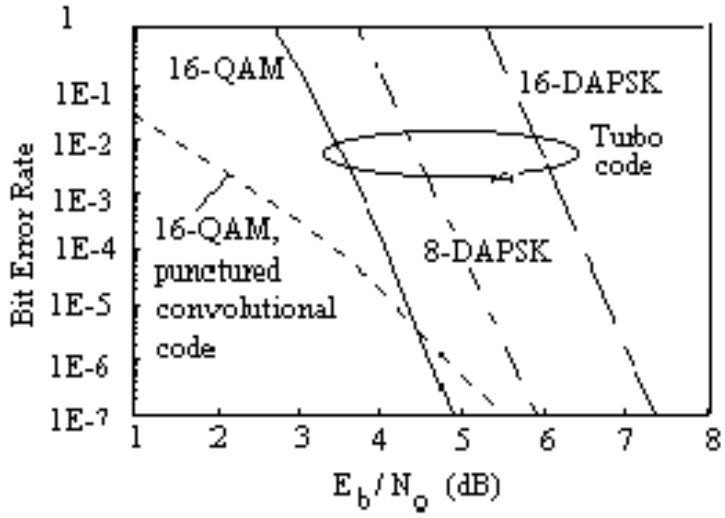

(b) Code rate = ½

Fig. (3) Performance of different modulation schemes in an AWGN channel

IV. TRANSMISSION OF HIGHER BIT RATE

The error performance of circular 16–DAPSK with Turbo code has been analyzed for an AWGN and frequency–selective Rayleigh fading channels. The numerical results have shown that although the error probability of circular 16–DAPSK is slightly worse when compared with 16–QAM under the same bit rate transmission, it is superior when compared with 64–DAPSK with 4 times bit rate compared with 16–DAPSK. Suppose the transmission bandwidth is fixed for the two cases of 16 and 64–DAPSK. So, for the same bandwidth, 64–DAPSK can carry 4 times the bit rate of 16–DAPSK. This implies to use higher bit rate transmission over the same channel bandwidth [2].

In many applications, the desired data rate far exceeds the available bandwidth. In such cases, it is necessary to increase the spectral efficiency of the communication system. Increasing the size of the signaling constellation does this; the symbol transmission rate (and thus the Nyquist bandwidth) remains the same, but the number of possible values taken on by each symbol is increased. Figure 5 shows the performance of 1/3 Turbo code rate over 16 and 64–DAPSK modulators with different bit rates (64–DAPSK modulator carries 4 kb/s information signal and channel coding whereas 16–DAPSK modulator carries 1 kb/s information signal)

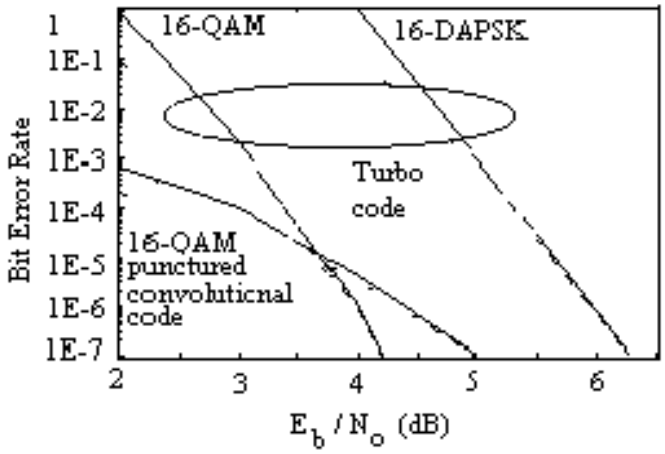

(a) code rate = 1/3

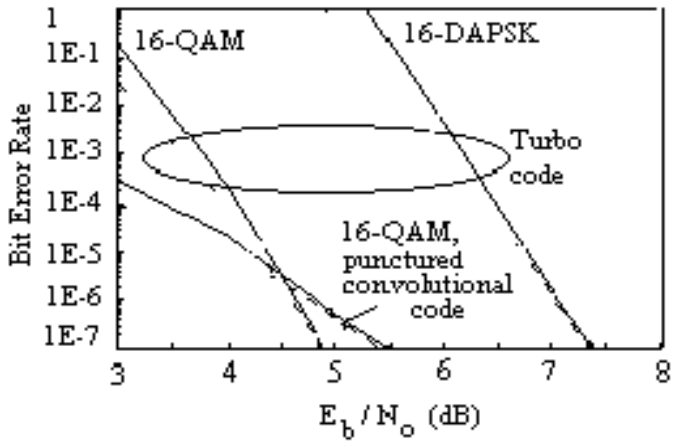

(b) code rate = 1/2

Fig. (4) Performance of 16–DAPSK modulation technique in frequency–selective Rayleigh fading channel

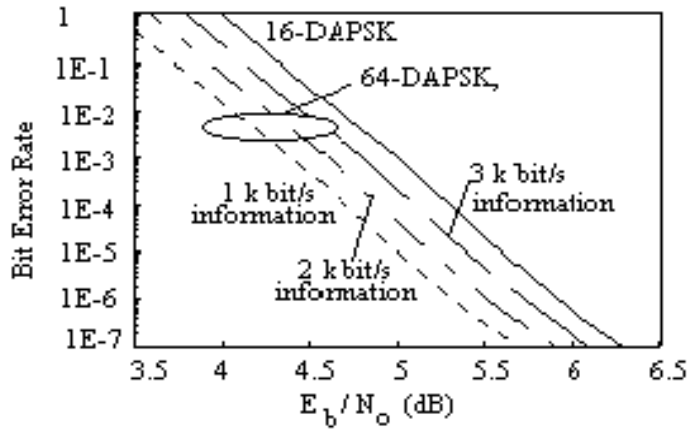

Fig. (5) Performance of 16 and 64–DAPSK modulators under the same transmission bandwidth

The simulation shows 64–DAPSK with 1 kb/s information signal and 3 kb/s channel coding is superior to 16–DAPSK modulator with 1 kb/s information signal by approximately 0.3 dB. From the figure, it is shown that in 64–DAPSK, as the information bits is increasing; the performance becomes comparable with 16–DAPSK modulator because of the decreasing in the bits of encoding in the transmitted signal.

V. CONCLUSION

For coherent systems, Turbo codes have been shown to be bandwidth efficient scheme offering large gains over un–coded schemes with only modest receiver complexity. There has been good deal of interest recently in applying Turbo codes to channels in which it is difficult, if not impossible, to obtain phase coherence. Examples of this type of channel are cellular radio systems, Time Division Multiple Access (TDMA) systems and frequency hopping systems. In all of these cases, it is difficult to operate coherently because of the high demands that are placed on the receiver to quickly acquire the phase of the received signal. DAPSK transmission and non–coherent detection is an attractive technique in this environment as it obviates the need for and difficulties associated with phase lock synchronizers, so only frequency tracking is necessary. A large enough observation shows that non–coherent systems can approach the performance of coherent systems.

In this paper, high data–rate systems applied in multi–path propagation digital radio broadcasting channels with different maximum Doppler frequency spread have been considered. The presented 16–DAPSK–modulation technique uses the phase and simultaneously the amplitude for differential modulation. The difference in the performance between the coherence and the differential modulation technique are in the order of approximately 2.5 dB in E_b/N_o for BER of 10^{-5} for Turbo coded case in AWGN and Rayleigh fading channels. The situation shows simple technical trade–off where small degradation in performance but large difference in computation complexity and robustness occurs.

APPENDIX 1

This appendix briefly describes the 16–DAPSK modulation/demodulation scheme and the theoretical characteristics in the AWGN channel. For other levels like 8, 32 and 64, it is a straightforward application.

16–DAPSK modulation is a combination of 8–DPSK (Differential Phase Shift keying) and 2–DASK (Differential Amplitude Phase Shift). Figure 6 shows the constellation diagram for 16–DAPSK–modulation scheme. Basically, differential modulation scheme requires approximately 3 dB more power in AWGN channel to achieve the same BER performance as the coherent modulation scheme. In addition, the constellation of 16–DAPSK does not have an optimum distance between points, so this modulation scheme has loss of about 1.5 dB in power in comparison with the ordinary square 16–QAM [10].

The output of the encoder is organized into sets of four–bit binary data $c_k^{(0)}, c_k^{(1)}, c_k^{(2)}, c_k^{(3)}$. These data are mapped into the complex value s_k

$$s_k = r_k \exp(j\Delta\varphi_k) \tag{1.1}$$

where r_k and $\Delta\varphi_k$ represent amplitude transition factor and phase transition factor, respectively. The phase transition factor $\Delta\varphi_k$ in the transmitted complex value s_k means applying Gray mapping of three–bit binary data $c_k^{(0)}, c_k^{(1)}, c_k^{(2)}$ for 8–DPSK modulation according to Table 1. The remaining binary data $c_k^{(3)}$ is mapped in two rings in constellation diagram of 16–DAPSK modulation signals [5]. For each transmitted signal, the amplitude transition factor r_k in Table 2 is multiplied by a_{k-1}, which is the amplitude of previous transmitted complex symbols. A ring factor α in 16–DAPSK modulation is defined as

$$\alpha = a_H/a_L \tag{1.2}$$

where a_L and a_H $(a_L < a_H)$ represents the two amplitude levels of the modulated signals. Therefore, the

transmitted complex symbol d_k is [10]

$$d_k = a_k \exp(j\varphi_k) = s_k d_{k-1} = r_k \exp(j\Delta\varphi_k) * a_{k-1} \exp(j\varphi_{k-1}) = r_k a_{k-1} \exp[j(\Delta\varphi_k + \varphi_{k-1})] \quad (1.3)$$

where d_{k-1} represents the previously transmitted complex symbols.

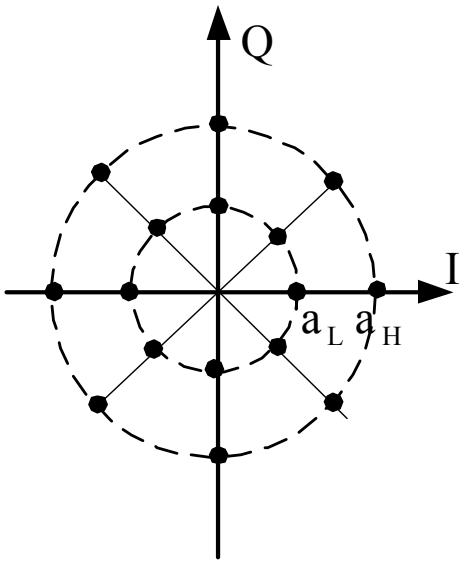

Fig. (6) Signal constellation of 16–DAPSK modulator

Table 1 Phase transition

$\Delta\varphi_k$	$c_k^{(0)}$	$c_k^{(1)}$	$c_k^{(2)}$
0	0	0	0
π/4	0	0	1
π/2	0	1	1
3π/4	0	1	0
π	1	1	0
5π/4	1	1	1
3π/2	1	0	1
7π/4	1	0	0

To obtain the differential complex value s_k, the received complex symbol $\hat{d}_k$ is divided by the previous received complex symbol $\hat{d}_{k-1}$

$$\hat{s}_k = \hat{d}_k / \hat{d}_{k-1} = (\hat{a}_k / \hat{a}_{k-1}) \exp[j(\hat{\varphi}_k - \hat{\varphi}_{k-1})] = \hat{r}_k \exp(j\Delta\hat{\varphi}_k) \quad (1.4)$$

where $\hat{r}_k$ and $\Delta\hat{\varphi}_k$ represent the amplitude ratio and phase rotation, respectively.

Table 2 Amplitude transition

r_k		$c_k^{(3)}$	
		0	1
a_{k-1}	a_L	1	α
	a_H	1	1/α

The estimated three bit binary data $\hat{c}_k^{(0)}, \hat{c}_k^{(1)}, \hat{c}_k^{(2)}$ are given by demapping the received phase rotation value $\Delta\hat{\varphi}_k$ according to Table 1. To get the binary data $\hat{c}_k^{(3)}$ on 2–DASK, the received amplitude ratio $\hat{r}_k$ is compared with the threshold values β_L and β_H $(\beta_L < \beta_H)$. If the received amplitude ratio is

$$\beta_L < \hat{r}_k < \beta_H \tag{1.5}$$

the received data $\hat{c}_k^{(3)}$ is decided as logic 0, otherwise logic 1. The threshold for 2–DAPSK [11] is

$$\beta_L = 2/(1+\alpha), \quad \beta_H = (1+\alpha)/2 \tag{1.6}$$

Figure 7 shows the constellation diagram for the 8 and 32–DAPSK modulation schemes.

When the bit error are caused by AWGN channel, the theoretical bit error probability of M–DAPSK modulation scheme can be approximated by the average BER of M_1–DPSK and M_2–DASK, where $M = M_1 * M_2$.

For M–DAPSK, the average BER $(P_{M-DAPSK})$ in AWGN channel is [12]

$$P_{M-DAPSK} = \frac{1}{\log_2 M}\left[\log_2 M_1 \left(P_{M_1-DPSK}\right) + \log_2 M_2 \left(P_{M_2-DASK}\right)\right] \tag{1.7}$$

where P_{M_1-DPSK} and P_{M_2-DASK} are the average BERs of M_1–DPSK and M_2–DASK in AWGN channel. The average BER of M_1–DPSK (P_{M_1-DPSK}) is [12]

$$P_{M_1-DPSK} = \frac{1}{2}\left[\frac{1}{\log_2 M_1} Q\left\{\frac{2}{\sqrt{1+\alpha^2}}\sqrt{\frac{S}{N}}\sin\left(\frac{\pi}{\sqrt{2}M_1}\right)\right\} + \frac{1}{\log_2 M_1} Q\left\{\frac{2\alpha}{1+\alpha^2}\sqrt{\frac{S}{N}}\sin\left(\frac{\pi}{\sqrt{2}M_1}\right)\right\}\right] \tag{1.8}$$

where Q (.) is the Q–function and S/N represents the carrier–to–noise ratio of the signal.

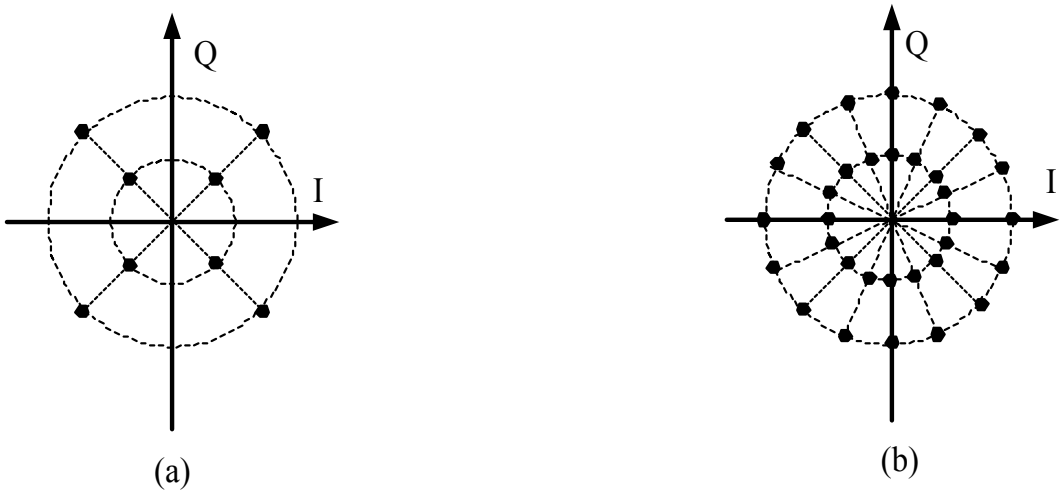

Fig. (7) Signal constellation of (a) 8–DAPSK (b) 32–DAPSK

The equivalent symbol distance P_{M_2-DASK} in M_2–DASK is given [13]

$$d_{M_2-DASK} = \frac{a_H - a_L}{\sqrt{1+\left(1+\alpha^2\right)^2/4}} \tag{1.9}$$

The BER of M_2–DASK (P_{M_2-DASK}) is

$$P_{M_2-DASK} = Q\left(\frac{\alpha-1}{\sqrt{1+\alpha^2}}\sqrt{\frac{E_b}{N_o\left[1+\left(1+\alpha^2\right)/4\right]}}\right) \tag{1.10}$$

Substituting Equation. (1.8) and (1.10) into Equation (1.7) gives the average BER of M–DAPSK in AWGN channel.

APPENDIX 2

The bit error probability of (n,k) linear block code observed through an AWGN channel satisfies the union bound [2]

$$P_b \le \sum_{i=1}^{2^k-1}\frac{\omega(m_i)}{k}Q\left(\sqrt{2r\omega(x_i)\frac{E_b}{N_o}}\right) \tag{2.1}$$

and assuming maximal likelihood decoding. E_b is the energy per bit, N_o is the one–sided noise power spectral density, $r = k/n$ is the code rate and $\omega(m_i)$ is the Hamming weight of the message m_i. Computing Equation. (2.1) requires the knowledge of weights of all 2^k–1 nonzero code words and their corresponding messages, and has a computational complexity that precludes its use for all but the smallest values of k. The number of terms in Equation (2.1) can be greatly reduced by gathering terms that produce the same code word weights

$$P_b \le \sum_{d=d_{min}}^{n}\frac{\tilde{\omega}_d N_d}{k}Q\left(\sqrt{2rd\frac{E_b}{N_o}}\right) \tag{2.2}$$

where N_d is the number of code words of weight d and $\tilde{\omega}_d$ is the average weight of N_d messages which produce weight d code words. At high SNRs, the bit error probability is approximated by the first term of Equation (2.2)

$$P_b \approx \frac{\tilde{\omega}_{d_{min}} N_{d_{min}}}{k}Q\left(\sqrt{2rd_{min}\frac{E_b}{N_o}}\right) \tag{2.3}$$

which is called the minimum distance asymptote.

The goal of code design has traditionally been to maximize d_{min}. With Turbo codes, however, the emphasis is to instead minimize the coefficient $\tilde{\omega}_{d_{min}} N_{d_{min}}/k$. Consider, for example, Turbo code composed of two $K_c = 5$ RSC (Recursive Systematic Convolution) encoders with feed–forward generator $(21)_8$ and feedback generator $(37)_8$, where the subscript 8 is the octal number. The interleaver size is L = 65536. Assume r = 1/2 and only the trellis of the upper encoder is terminated. Thus, this is (131072,65532)–block code. In [14], it is reported that the minimum distance of this code is $d_{min} = 6$, the number of free distance code words is on the average $N_{d_{min}} = 4.5$ and the average weight of the messages associated with the minimum distance code words is $\tilde{\omega}_{d_{min}} = 2$. Therefore, the minimum distance asymptote for this code is

$$P_b \approx \frac{(4.5)(2)}{65532}Q\left(\sqrt{6\frac{E_b}{N_o}}\right) \tag{2.4}$$

Now, consider the asymptotic performance of convolution code of similar decoder complexity. Because the block length of convolution codes is unbounded, Equation (2.2) does not apply. Instead, the following bound is used for the maximal likelihood decoding of convolution code [15]

$$P_b = \sum_{d=d_{free}}^{\infty}\omega_d^Q Q\left(\sqrt{2rd\frac{E_b}{N_o}}\right) \tag{2.5}$$

where ω_d^Q is the sum of the weights of all messages with $m_0 = 1$ and whose associated code words have weight d. At high SNR, the bit error probability of convolution code is approximated by the free distance asymptote

$$P_b \approx \omega^{Q}_{d_{free}} Q\left(\sqrt{2rd_{free}\frac{E_b}{N_o}}\right) \tag{2.6}$$

The decoder complexity of r = 1/2, $K_c = 15$ convolution code presented in [16] is approximately the same as that of r = 1/2, $K_c = 5$ Turbo code. For this convolution code, $d_{free} = 18$ and $\omega^{Q}_{d_{free}} = 187$ and thus the free distance asymptote is

$$P_b \approx 187Q\left(\sqrt{18\frac{E_b}{N_o}}\right) \tag{2.7}$$

Note the distinction between Equations. (2.3) and (2.7). The argument of Q–function is much larger for convolution code than that for Turbo code, and therefore, it can be expected that the slope of convolution code's asymptote will be much steeper than that for Turbo code. However, the coefficient preceding Q–function is much smaller for Turbo code than that for convolution code. Therefore, for sufficiently small E_b/N_o, it should be expected that Turbo code's asymptote would be lower than that of convolution code.

APPENDIX 3

The block diagram for a Turbo coded systems operating over an AWGN and Rayleigh fading channels as described in [1] is shown in Fig. 8. A sequence $\{m_i\}$, $0 \le i \le L-1$, $\{x_l\}$, $0 \le l \le L/r-1$, are passed to a channel interleave, which is implemented by writing the code bits row into a M_b by N_b matrix and reading the interleaved code bits $\{\tilde{x}_l\}$ from the matrix column–wise. The purpose of the interleave is to break up burst errors induced by the correlated fading channel. The interleaved bits are passed to a signal mapped, which creates a stream of symbols $\{v_n\}$, $0 \le n \le N-1$, which is a DAPSK modulation (described in Appendix 1), where N = L/r. The symbols are passed through a pulse–shaping filter, which has an impulse response g(t), and the resulting signal

$$s(t) = \sum_{n=0}^{N-1} v_n g(t - nT_s) \tag{3.1}$$

is transmitted over the complex base band channel, where v_n is the output of the symbol mapped and T_s is the symbol period. The energy per symbol is

$$E_s = \int_{-\infty}^{\infty} |g(t)|^2 dt \tag{3.2}$$

and the energy per bit is $E_b = \frac{N}{L}E_s$ (3.3)

The transmitted signal s(t) passes through a noisy channel consists of an AWGN and a Rayleigh fading channels with a multi–path because the surface of the earth and the ionosphere are involved in the mechanism of electromagnetic wave propagation. The channel output is

$$y(t) = \sum_{k=1}^{n} \rho_k c_k s(t - \Delta_k) \tag{3.4}$$

where ρ_k is the attenuation of the path number k listed in Table 3, Δ_k is the relative delay of the path number k listed in Table 3, and the time–variant tap weight $\{c_k(t)\}$ is zero mean complex–valued stationary Gaussian random processes. The magnitude $|c_k(t)|$ is Rayleigh distributed and the phase $\varphi(t)$ is uniformly distributed [1] and n is the number of the paths.

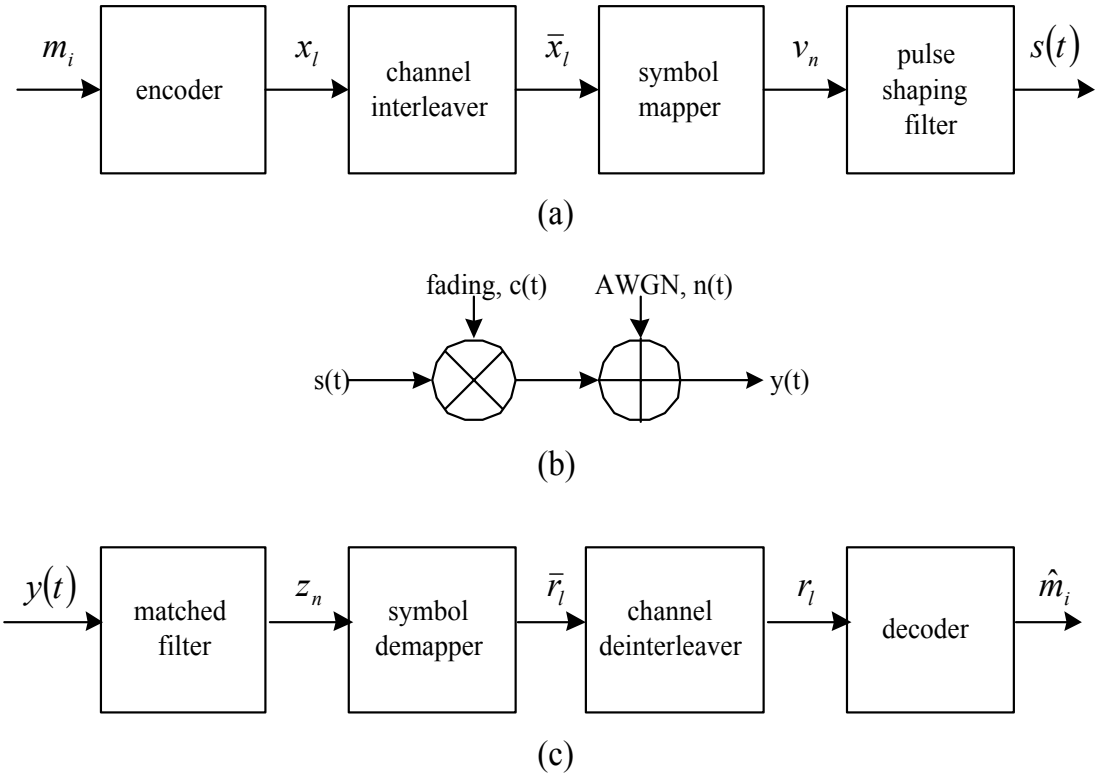

Fig. (8) Turbo coded system operating over a noisy channel (a) transmitter (b) noisy channel (c) receiver

Table 3 Different types of channels

	path 1	path 2	path 3	path 4
delay (Δ_k) (ms)	0	0.7	1.5	2.2
path gain, (ρ_k) (rms)	1	0.7	0.5	0.25
Doppler shift (D_{sh}) (Hz)	0.1	0.2	0.5	1.0
Doppler spread (D_{sp}) (Hz)	0.1	0.5	1.0	2.0

The received signal y(t) is passed through a matched filter with impulse response $g(T_s - t)$. The output of the matched filter is sampled at the symbol rate $1/T_s$ to produce the samples z_n. For DAPSK, the demapper produces the output $\tilde{r}_l$, which is then passed through a deinterleave to produce $\{r_l\}$. It is introduced at the input of a Turbo decoder. The turbo decoder performs Q–iterations of log–MAP decoding and produces the estimate $\{\hat{m}_i\}$ of the message. The length of the interleave L = 1024 is randomly generated and 5 iterations of improved iterative decoding are performed at the receiver.

REFERENCES

1. Itu–R Circular Letter 10/lcce/39, (1999, September).
2. Proakis, J. G. (1995),"Digital Communication", New York: Mcgraw–Hill.
3. Lu, J., Letaief, K. B., Chuang, J. C–I, and Liou, M. L. (1999), "M–PSK And M–QAM Computation using Signal–Space Concepts", IEEE Transactions on Communication, Vol. 47, No. 2, pp. 181–184.
4. Rowitch, D. N., and Milstein, L. B. (2000), "On the Performance of Hybrid FEC/ARQ Systems using Rate Compatible Punctured Turbo (RCPT) Codes", IEEE Transactions on Communication, Vol. 48, No. 6, pp. 948–

959.
5. May, T., and Rohling, H. (2000), "Turbo Detection of Convolutionally Coded and Differentially Modulated Signals", Signal Processing, Vol. 80, No. 2, pp. 349–355.
6. Lapidoth, A., and Sallaway, P. J. (2000), "Convolution Encoders to Minimize Bit–Error–Rate", European Transactions on Telecommunication, Vol. 11, No. 3, pp. 263–269.
7. Berrou, C., Glavieux, A., And Thitimajshima, P. (1993, May), "Near Shannon Limit Error–Correcting Coding and Decoding: Turbo–Codes (1)", Proceeding of IEEE International Conference on Communication, Geneva, Switzerland, pp. 1064–1070.
8. Valenti, M. C. (1999), "Iterative Detection and Decoding for Wireless Communications", Ph.D. Thesis, Faculty of Engineering, Virginia Polytechnic Institute and State University, Blacksburg, Virginia, U.S.A.
9. Sayhood, K. H., Ling, Z. G., and Nan, W. L. (2001), "Performance Analysis of Punctured Convolution Codes and Turbo–Codes", Electronics and Communication Engineering Journal, Vol. 13, No. 4, pp. 166–172.
10. Gerstacker, W. H., Schober, R., and Huber, J. B. (1999), "Decision–Feedback Differential Detection for 16 DAPSK Transmitted Over Ricean Fading Channels", Proceeding of IEEE Vehicular Technology Conference, Vtc'96, 50th IEEE, pp. 2515–2519.
11. Webb, W. T., Hanzo, L., and Steele, R. (1991), "Bandwidth Efficient QAM Schemes for Rayleigh Fading Channels", IEEE Proceeding I, Vol. 138, No. 3, pp. 169–175, September 19–22
12. Suzuki, T., and Mizuno, T. (1994, March), "Multiple–Symbol Differential Detection Scheme for Differential Amplitude Modulation", Proceeding of the International Zurich Seminar on Digital Communication, Izs'94, Zurich, Switzerland, pp. 326–337.
13. Bhargava, V. K., Haccoun, D., Matyas, R., and Nuspl, P. P. (1981), "Digital Communications by Satellite", New York: John Wiley & Sons.
14. Seghers, J. (1995), "On the Free Distance of Turbo Codes and Related Product Codes", Ph.D. Thesis, Swiss Federal Institute of Technology, Zurich, Switzerland.
15. Perez, L. C., Seghers, J., and Costello, D. J. (1996), "A Distance Spectrum Interpretation of Turbo Codes", IEEE Transactions on Information Theory, Vol. 42, No. 11, pp. 1698–1709.
16. Collins, O. M. (1992), "The Subtleties and Intricacies of Building a Constraint Length 15 Convolution Decoder", IEEE Transactions on Communication, Vol. 40, No. 12, pp. 1810–1819.